University of Reading

Identification of fractional-order transfer functions using exponentially modulated signals with arbitrary excitation waveforms

Article

Accepted Version

Creative Commons: Attribution-Noncommercial-No Derivative Works 4.0

Galvão, R. K. H., Tiexeira, M. C. M., Assunção, E., Paiva, H. M. and Hadjiloucas, S. ORCID: https://orcid.org/0000-0003-2380-6114 (2020) Identification of fractional-order transfer functions using exponentially modulated signals with arbitrary excitation waveforms. ISA Transactions, 103. pp. 10-18. ISSN 0019-0578 doi: 10.1016/j.isatra.2020.03.027 Available at https://centaur.reading.ac.uk/89796/

It is advisable to refer to the publisher's version if you intend to cite from the work. See Guidance on citing.

To link to this article DOI: http://dx.doi.org/10.1016/j.isatra.2020.03.027

Publisher: Elsevier

All outputs in CentAUR are protected by Intellectual Property Rights law, including copyright law. Copyright and IPR is retained by the creators or other copyright holders. Terms and conditions for use of this material are defined in the End User Agreement.

www.reading.ac.uk/centaur

University of Reading

CentAUR

Central Archive at the University of Reading

Reading's research outputs online

Identification of fractional-order transfer functions using exponentially modulated signals with arbitrary excitation waveforms

Roberto Kawakami Harrop Galvão

Department of Electronic Engineering, Instituto Tecnológico de Aeronáutica (ITA), São José dos Campos, SP, Brazil

Marcelo Carvalho Minhoto Teixeira, Edvaldo Assunção

Department of Electrical Engineering, São Paulo State University (UNESP), Ilha Solteira, SP, Brazil

Henrique Mohallem Paiva

Institute of Science and Technology, Universidade Federal de São Paulo (UNIFESP), São José dos Campos, SP, Brazil

Sillas Hadjiloucas*

School of Biological Sciences, Department of Biomedical Engineering, The University of Reading, Reading RG6 6AY, United Kingdom

Abstract

This paper proposes a new identification method based on an exponential modulation scheme for the determination of the coefficients and exponents of a fractional-order transfer function. The proposed approach has a broader scope of application compared to a previous method based on step response data, in that it allows for the use of arbitrary input signals. Moreover, it dispenses with the need for repeated simulations during the search for the best fractional exponents, which significantly reduces the computational workload involved in the identification process. Two examples involving measurement noise at the observed system output are presented to illustrate the effectiveness of the proposed method when compared to a conventional output-error optimization approach based on the polytope algorithm. In both examples, the proposed method is found to provide a better trade-off between computational workload and accuracy of the parameter estimates for different realizations of the noise.

Keywords: Fractional order systems, system identification, transfer functions

1. Introduction

Over the past 20 years there has been a surge in the development of fractional order modelling tools for the emulation of complex processes with greater accuracy compared to conventional integer order representations. This has led to an increased interest in the application of fractional order calculus across all branches of sciences, from biology and medicine [1], [2], [3] to mechatronics [4], [5], [6]. Within the circuits and systems community, new opportunities have arisen for the analysis of complex 2-port networks [7] and passive electrical networks composed of fractional elements [8], [9], which also enabled novel control design solutions with improved stability while using fewer components [10]. In addition, many of these design solutions are very promising in the modelling and control

*Corresponding author
Email address: s.hadjiloucas@reading.ac.uk (Sillas Hadjiloucas*)

of physicochemical processes associated with energy storage [11], [12], [13]. Fractional order modelling has also been particularly useful in the study of dielectrics [14], [15], [16], [17], [18], as well as viscoelasticity [19], [20], [21] and heat transfer [22], [23], [24]. Moreover, within a system-theoretic framework, much research has been devoted to the stability analysis [25], [26], [27] and control [28], [29], [30] of fractional order systems.

A fundamental problem often addressed through measurements or simulations is the identification of a fractional order model that suitably describes the dynamics of the system under investigation. Given a set of time-domain input-output data, a standard identification procedure consists of using a discrete-time approximation for the fractional-order derivative operation in order to cast the problem into a regression form [31]. Such an approximation can be obtained e.g. by using a truncated Grunwald-Letnikov series [32] or digital FIR (finite impulse response) filters [33]. Nevertheless, this procedure assumes that the fractional exponents are known a priori, which may be too strong an assumption in practical applications. Alternatively, the coefficients and fractional exponents can be grouped into a parameter vector to be optimized by using a numerical search method. The goal then consists of minimizing some metric of the difference between the actual system response and the model output obtained by simulation [31]. However, this approach may be computationally demanding because several simulations will have to be carried out as the parameter vector is varied during the search procedure. An alternative to circumvent this problem was proposed in [34]. By approximating the input and output signals as linear combinations of Haar wavelets, the model output could be written as an algebraic expression involving the model coefficients and exponents. However, a numerical search method was still required to determine the optimal parameter estimates.

In the case of fractional order transfer functions of the form $G(s) = b/(1 + as^{\alpha})$, [35] proposed an identification method which enabled the determination of the coefficients k, T and the exponent α through a simple iterative procedure involving fractional order integration. However, the proposed method was only applicable to step response data. This can be a shortcoming in practice, as there are cases where a step input with large magnitude would be required to obtain output measurements with suitable signal-to-noise ratio, which may be prohibitive due to slew rate constraints of the excitation source or possible damage to the system under test.

In view of these limitations, the present paper proposes a new identification method, which is developed as an extension of a previous step response procedure [36] for the case of arbitrary input signals. For transfer functions of the form $G(s) = b/(1 + as^{\alpha})$, the proposed method allows for the full analytical determination of the parameters a, b, α, without the need for numerical optimization. In the case of transfer functions with additional parameters, a novel evaluation index is employed in the search for the best fractional exponents, as an alternative to the error between the model response and the system output. The new evaluation index dispenses with the need for repeated simulations of the fractional-order model, which significantly reduces the computational workload involved in the identification process.

1.1. Notation

Herein the following notation will be employed. The Laplace transform of $y(t)$, $t \geq 0$, will be denoted by $Y(s) = \mathcal{L}[y(t)]$. Definitions will be stated by using the $\triangleq$ symbol. The limit value of $y(t)$ will be denoted as $y(\infty) \triangleq \lim_{t\to\infty} y(t)$.

2. Preliminary result

It is assumed that the system under consideration can be described by a transfer function of the form

$$G(s) = \frac{b_0 + b_1 s^{\beta_1} + \cdots + b_m s^{\beta_m}}{1 + a_1 s^{\alpha_1} + \cdots + a_n s^{\alpha_n}} \tag{1}$$

where the coefficients $b_0, b_1, \ldots, b_m, a_1, \ldots, a_n$ and the positive real-valued exponents $\beta_1, \ldots, \beta_m, \alpha_1, \ldots, \alpha_n$ are parameters to be identified.

The proposed identification method is based on the generation of two auxiliary signals $z(t)$ and $w(t)$, which depend on a positive real-valued constant σ, as depicted in Fig. 1. As can be seen, the generation of these signals involves a time-domain multiplication by an exponential function $e^{-\sigma t}$, which can be regarded as a modulation scheme in a broad sense. A similar exponential modulation procedure was employed in [36], but the proposed identification method was restricted to the use of a step signal in the input $u(t)$. Herein, arbitrary input waveforms can be employed.

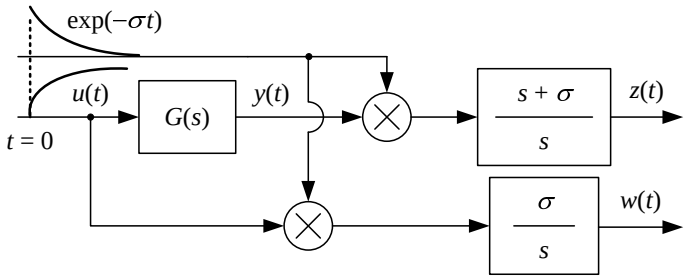

Figure 1: Generation of the signals employed in the proposed identification method. The rectangular blocks correspond to transfer functions, whereas the circle with a × sign indicates a pointwise multiplication of the signals in the time domain.

Theorem 1 below establishes a relation between the steady-state values $z(\infty)$, $w(\infty)$ and the parameters of the transfer function $G(s)$ in (1). This theorem cannot be directly derived from the mathematical formulation in [36], which was restricted to the use of a step input signal. Therefore, a proof will be presented.

Theorem 1: If $\sigma > 0$ is such that the limits

$$z(\infty) \triangleq \lim_{t\to\infty} z(t)\ , \quad w(\infty) \triangleq \lim_{t\to\infty} w(t) \tag{2}$$

exist, then the following identity holds:

$$z(\infty) = w(\infty)\frac{b_0 + b_1 \sigma^{\beta_1} + \cdots + b_m \sigma^{\beta_m}}{1 + a_1 \sigma^{\alpha_1} + \cdots + a_n \sigma^{\alpha_n}} \tag{3}$$

Proof: The Laplace transform of the system response $y(t)$ is given by

$$Y(s) = G(s)U(s) \tag{4}$$

The first auxiliary signal $z(t)$ in Fig. 1 is the result of passing $y(t)e^{-\sigma t}$ through a filter with transfer function $(s+\sigma)/s$, i.e.

$$Z(s) = \left(\frac{s+\sigma}{s}\right)\mathcal{L}[y(t)e^{-\sigma t}] = \left(\frac{s+\sigma}{s}\right)Y(s+\sigma) \tag{5}$$

where the last equality follows from the frequency-shifting property of the Laplace transform [37].

From (4) and (5) it follows that

$$Z(s) = \left(\frac{s+\sigma}{s}\right) G(s+\sigma)U(s+\sigma) \tag{6}$$

In view of the Final Value Theorem, which is also valid for fractional calculus [38], $z(\infty)$ can be related to $Z(s)$ as

$$z(\infty) = \lim_{s\to 0} sZ(s) \tag{7}$$

From (6) and (7), it can be concluded that

$$z(\infty) = \sigma G(\sigma)U(\sigma) \tag{8}$$

Similary, the Laplace transform of the second auxiliary signal $w(t)$ in Fig. 1 is given by

$$W(s) = \frac{\sigma}{s}\mathcal{L}[u(t)e^{-\sigma t}] = \frac{\sigma}{s}U(s+\sigma) \tag{9}$$

From (9) and the Final Value Theorem, one obtains

$$w(\infty) = \lim_{s\to 0} sW(s) = \sigma U(\sigma) \tag{10}$$

From (8) and (10) it follows that

$$z(\infty) = w(\infty)G(\sigma) \tag{11}$$

Finally, from (1) and (11), one arrives at (3), *qed* □

In what follows, Theorem 1 will be initially employed to derive an identification procedure for a transfer function $G(s)$ with a single fractional exponent. Afterwards, the general case will be handled.

3. Single fractional exponent

Consider a transfer function of the following form:

$$G(s) = \frac{b}{1+as^{\alpha}} \tag{12}$$

This is a particular case of (1), with $n = 1$ and $m = 0$. For brevity of notation, b_0, a_1 and α_1 are denoted by b, a and α, respectively. From (3) in Theorem 1, it follows that

$$z(\infty) = w(\infty)\frac{b}{1+a\sigma^{\alpha}} \tag{13}$$

for any $\sigma > 0$ such that the limits (2) exist. Assume that this is the case for $\sigma_1 > 0$, $\sigma_2 = \sigma_1^{1/2}$ and $\sigma_3 = \sigma_1^{1/4}$, with $\sigma_1 \neq 1$. In view of (13), one can write

$$z_1(\infty) = \frac{w_1(\infty)b}{1+a\sigma_1^{\alpha}}\ ,\quad z_2(\infty) = \frac{w_2(\infty)b}{1+a\sigma_1^{\alpha/2}}\ ,\quad z_3(\infty) = \frac{w_3(\infty)b}{1+a\sigma_1^{\alpha/4}} \tag{14}$$

where $z_i(\infty)$ and $w_i(\infty)$ denote the values of $z(\infty)$ and $w(\infty)$ obtained by using the block diagram in Fig. 1 with σ_i $(i = 1, 2, 3)$ in place of σ. It is worth noting that the input and output data only need to be acquired once, because the same $u(t)$ and $y(t)$ signals are used for the calculation of all $z_i(\infty)$ and $w_i(\infty)$ values.

From (14), it follows that

$$az_1(\infty)\sigma_1^{\alpha} = w_1(\infty)b - z_1(\infty) \tag{15}$$

$$az_2(\infty)\sigma_1^{\alpha/2} = w_2(\infty)b - z_2(\infty) \tag{16}$$

$$az_3(\infty)\sigma_1^{\alpha/4} = w_3(\infty)b - z_3(\infty) \tag{17}$$

From (15) and (16), one can write

$$a\frac{[z_2(\infty)]^2}{z_1(\infty)} = \frac{[w_2(\infty)b - z_2(\infty)]^2}{w_1(\infty)b - z_1(\infty)} \tag{18}$$

whereas from (16) and (17), one arrives at

$$a\frac{[z_3(\infty)]^2}{z_2(\infty)} = \frac{[w_3(\infty)b - z_3(\infty)]^2}{w_2(\infty)b - z_2(\infty)} \tag{19}$$

From (18) and (19), it follows that

$$\frac{[w_2(\infty)b - z_2(\infty)]^2}{w_1(\infty)b - z_1(\infty)}\frac{z_1(\infty)}{[z_2(\infty)]^2} = \frac{[w_3(\infty)b - z_3(\infty)]^2}{w_2(\infty)b - z_2(\infty)}\frac{z_2(\infty)}{[z_3(\infty)]^2} \tag{20}$$

which leads to

$$\begin{aligned}&\left\{[w_2(\infty)]^3 - \kappa w_1(\infty)[w_3(\infty)]^2\right\}b^3 + \left\{\kappa[w_3(\infty)]^2 z_1(\infty) + 2\kappa w_1(\infty)w_3(\infty)z_3(\infty) - 3[w_2(\infty)]^2 z_2(\infty)\right\}b^2 + \\ &\left\{3w_2(\infty)[z_2(\infty)]^2 - 2\kappa w_3(\infty)z_1(\infty)z_3(\infty) - \kappa w_1(\infty)[z_3(\infty)]^2\right\}b + \kappa z_1(\infty)[z_3(\infty)]^2 - [z_2(\infty)]^3 = 0\end{aligned} \tag{21}$$

where

$$\kappa = \frac{[z_2(\infty)]^3}{z_1(\infty)[z_3(\infty)]^2} \tag{22}$$

After solving the cubic equation (21) for b, the value of a can be obtained from (18) as

$$a = \frac{[w_2(\infty)b - z_2(\infty)]^2}{w_1(\infty)b - z_1(\infty)}\frac{z_1(\infty)}{[z_2(\infty)]^2} \tag{23}$$

Finally, the exponent α can be obtained from (15) as

$$\alpha = \frac{\ln\left(\dfrac{w_1(\infty)b - z_1(\infty)}{az_1(\infty)}\right)}{\ln\sigma_1} \tag{24}$$

4. General case

In the general case, Eq. (3) in Theorem 1 leads to

$$z(\infty) = w(\infty)\frac{b_0 + b_1\sigma^{\beta_1} + \cdots + b_m\sigma^{\beta_m}}{1 + a_1\sigma^{\alpha_1} + \cdots + a_n\sigma^{\alpha_n}} \tag{25}$$

which can be rewritten as

$$z(\infty)a_1\sigma^{\alpha_1} + \cdots + z(\infty)a_n\sigma^{\alpha_n} - w(\infty)(b_0 + b_1\sigma^{\beta_1} + \cdots + b_m\sigma^{\beta_m}) = -z(\infty) \tag{26}$$

Assume that tentative values are assigned to the fractional exponents $\alpha_1, \ldots, \alpha_n, \beta_1, \ldots, \beta_m$. By evaluating $z_i(\infty)$ and $w_i(\infty)$ with $q \geq (n+m+1)$ different values of σ_i ($i = 1, 2, \ldots, q$), Eq. (26) can be used to derive a system of linear equations of the form $A\theta = c$, with

$$A = \begin{bmatrix} z_1(\infty)\sigma_1^{\alpha_1} & \cdots & z_1(\infty)\sigma_1^{\alpha_n} & -w_1(\infty) & -w_1(\infty)\sigma_1^{\beta_1} & \ldots & -w_1(\infty)\sigma_1^{\beta_m} \\ z_2(\infty)\sigma_2^{\alpha_1} & \cdots & z_2(\infty)\sigma_2^{\alpha_n} & -w_2(\infty) & -w_2(\infty)\sigma_2^{\beta_1} & \ldots & -w_2(\infty)\sigma_2^{\beta_m} \\ \vdots & \vdots & \vdots & \vdots & \vdots & \vdots & \vdots \\ z_q(\infty)\sigma_q^{\alpha_1} & \cdots & z_q(\infty)\sigma_q^{\alpha_n} & -w_q(\infty) & -w_q(\infty)\sigma_q^{\beta_1} & \ldots & -w_q(\infty)\sigma_q^{\beta_m} \end{bmatrix}, \tag{27}$$

$$\theta = [a_1 \cdots a_n \, b_0 \, b_1 \cdots b_m]^T, \; c = -[z_1(\infty) \, z_2(\infty) \cdots z_q(\infty)]^T \tag{28}$$

The value of q should be at least equal to $(n + m + 1)$, so that the system of equations $A\theta = c$ is not underdetermined. However, it is advisable to use larger values of q in order to mitigate the effect of measurement noise. As a rule of thumb, the choice $q = 2(n + m + 1)$ is adopted in the present work. A least-squares estimate $\hat{\theta}$ for the model coefficients can then be calculated as

$$\hat{\theta} = (A^T A)^{-1} A^T c \tag{29}$$

provided that A is a full-rank matrix.

Now, let e be a column vector of residues defined as $e = c - A\hat{\theta}$. In view of (29), e can also be written as $e = [I - A(A^T A)^{-1} A^T]c$. Therefore, the sum square value of the residues can be expressed as

$$\begin{aligned} E = e^T e &= c^T [I - A(A^T A)^{-1} A^T][I - A(A^T A)^{-1} A^T]c = c^T [I - 2A(A^T A)^{-1} A^T + A(A^T A)^{-1} A^T]c \\ &= c^T [I - A(A^T A)^{-1} A^T]c \end{aligned} \tag{30}$$

The fractional-order exponents can then be estimated by minimizing E with respect to $\alpha_1, \ldots, \alpha_n, \beta_1, \ldots, \beta_m$, either by using a gridding procedure or guided search methods [39].

5. Results and Discussion

The results presented in this section were obtained by using the Matlab® software and the FOTF code available within the FOMCON toolbox (fomcon.net) for the simulation of fractional-order systems. More specifically, the fractional-order derivatives were implemented by using the Grunwald-Letnikov definition with a time step of 10^{-2} seconds, as described in [32]. The Matlab® software was also employed to carry out the multiplication and filtering operations presented in Fig. 1. Suitable values of σ_i, $i = 1, 2, \ldots, q$, were chosen in order to obtain a clear characterization of the limits $z_i(\infty)$ and $w_i(\infty)$, as will be described below.

For comparison, the polytope algorithm [39] implemented in the Matlab® Optimization Toolbox™ was used to estimate the coefficients and fractional exponents of the transfer function by minimizing the root-mean-square error (RMSE) between the system output y and the resulting model response. The default optimization settings of the toolbox were employed throughout. The computational times reported in the results were obtained with an i7-6700K processor and 24GB of RAM memory. Statistical plots were generated using the Matlab® Statistics Toolbox™.

5.1. Example 1

Consider a transfer function of the form (12) with $b = 2$, $a = 5$, and $\alpha = 1.5$, i.e.

$$G(s) = \frac{2}{1 + 5s^{1.5}} \tag{31}$$

The identification was carried out by using an input signal $u(t)$ given by

$$u(t) = \sin\left(\frac{\pi t}{10}\right) + \sin\left(\frac{\pi t}{15}\right) + \sin\left(\frac{\pi t}{20}\right) \tag{32}$$

which is shown in Fig. 2a. To simulate measurement imperfections, the output signal $y(t)$ was corrupted with additive Gaussian noise of zero mean and standard deviation of 0.1. The resulting signal is presented in Fig. 2b.

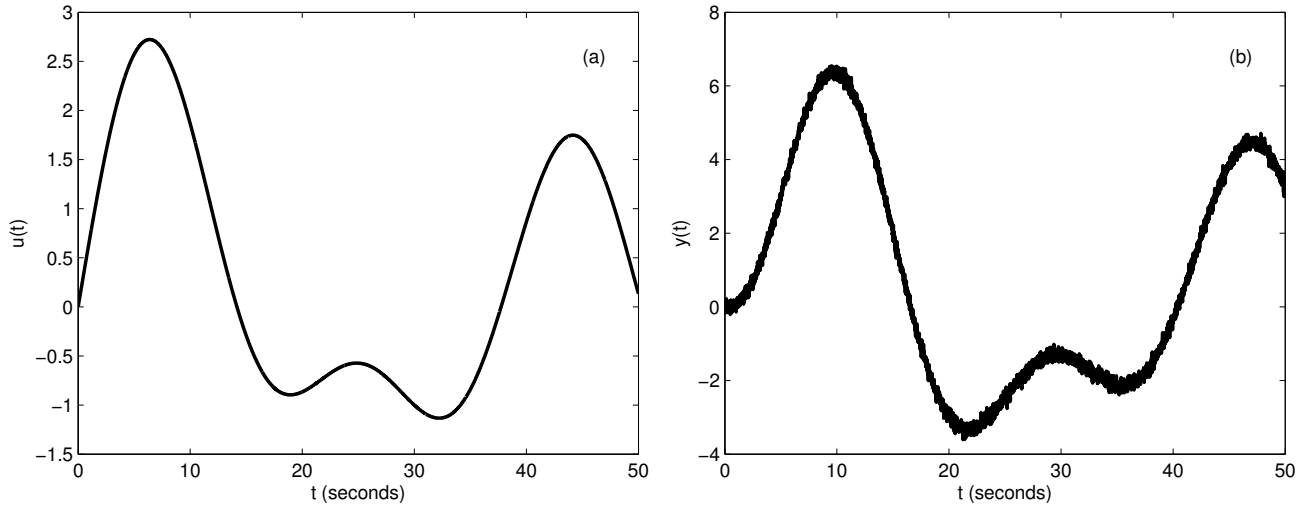

Figure 2: Example 1. (a) Input $u(t)$ and (b) output $y(t)$ signals employed in the identification.

In order to use the identification approach proposed in Section 3, a suitable value for σ_1 must be initially chosen. For this purpose, a preliminary analysis was carried out as follows. Let $\sigma = (\ln 100)/50 = 0.092$, which the value for which the exponential function $e^{-\sigma t}$ decays by a factor of 100 over the time range $[0, 50]$ seconds of the identification data. Fig. 3 presents the plots of $z_1(t)$ and $w_1(t)$ for five different values of σ_1, namely $\sigma/4$, $\sigma/2$, σ, 2σ and 4σ. As can be seen, the determination of the limit values $z_1(\infty)$ and $w_1(\infty)$ becomes more accurate as σ_1 is increased, owing to the faster convergence of the exponential function. However, the use of arbitrarily large values of σ_1 would not be advised, because the information conveyed by the latter parts of the $u(t)$ and $y(t)$ signals would be suppressed upon the multiplication by $e^{-\sigma_1 t}$. Therefore, the value $\sigma_1 = 2\sigma = 0.184$ was adopted as a compromise choice. In line with the procedure described in Section 3, the values of σ_2 and σ_3 were taken as $\sigma_2 = \sigma_1^{1/2} = 0.429$ and $\sigma_3 = \sigma_1^{1/4} = 0.655$. Since these values are larger than σ_1, they will not hamper the determination of the limit values $z_2(\infty)$, $w_2(\infty)$ and $z_3(\infty)$, $w_3(\infty)$.

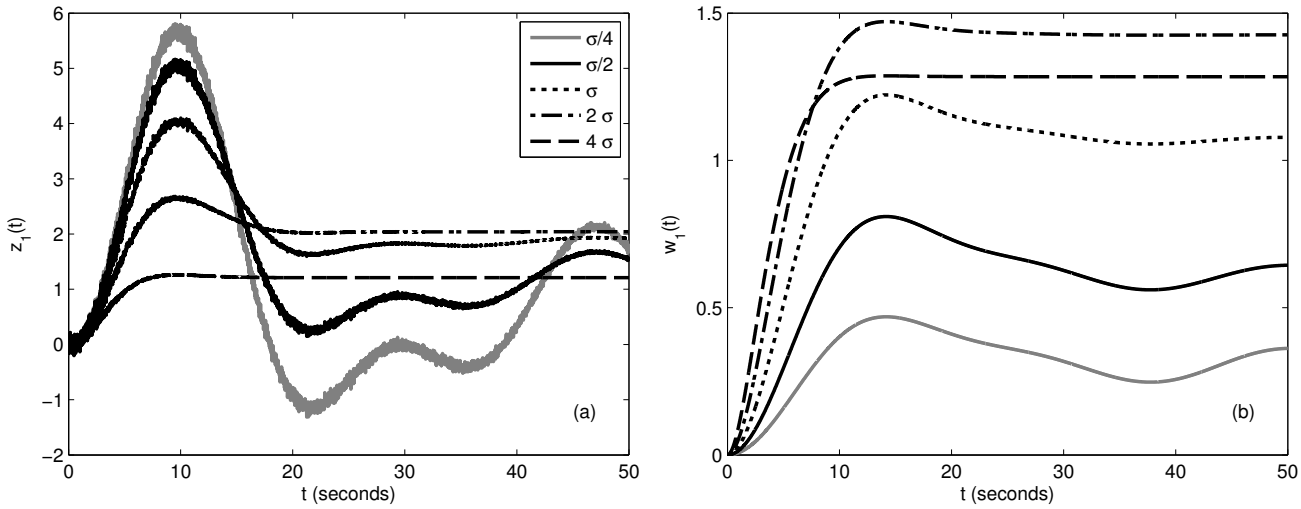

Figure 3: Example 1. Auxiliary signals $z_1(t)$ and $w_1(t)$ for five different values of σ_1.

Table 1: Identification results

b	a	α	δ_1	δ_2	δ_3
0	-1	0	*	*	*
0.63	-0.10	-1.01	2.2×10^{-16}	0	-0.37
2.00	5.01	1.50	0	-1.1×10^{-16}	-3.4×10^{-16}

*Invalid δ_i values because $1 + a\sigma_i^{\alpha} = 0$.

Table 1 presents the results associated to the three solutions of the cubic equation (21). In order to check conformity with (14), the following quantities were calculated:

$$\delta_i = \frac{z_i(\infty) - \dfrac{w_i(\infty)b}{1 + a\sigma_i^{\alpha}}}{z_i(\infty)}, \; i = 1, 2, 3 \tag{33}$$

The first two rows of the table correspond to invalid solutions, which arise because the derivation of (18), (19) from (15) - (17) and the derivation of (20) from (18), (19) involve squaring and ratioing operations, which may lead to sign ambiguities. The valid results are those in the last row of the table, for which δ_1, δ_2 and δ_3 are all approximately zero. Indeed, the identified parameters $b = 2.00$, $a = 5.01$ and $\alpha = 1.50$ match the corresponding values in (31), which illustrates the validity of the proposed approach even in the presence of measurement noise.

Table 2: Example 1. Parameter estimates (average ± standard deviation over 1000 realizations) and computational workload. MaxFunEvals is the upper bound on the number of cost function evaluations in the polytope algorithm.

Parameter	Proposed method	Polytope algorithm		Actual value
		MaxFunEvals = 10	MaxFunEvals = 40	
α	1.50 ± 0.03	1.4 ± 0.2	1.4 ± 0.1	1.5
a	4.98 ± 0.06	4.8 ± 1.5	4.7 ± 0.8	5
b	2.00 ± 0.02	2.1 ± 0.6	2.1 ± 0.2	2
Average computational workload (seconds)	6.5×10^{-4}	1.5	5.6	

To investigate the reproducibility of the results, the identification was repeated 1000 times, with different realizations of the measurement noise. The resulting values of average and standard deviation for the parameter estimates are presented in Table 2. As can be seen, the estimates are in close agreement with the actual parameter values, with relative standard deviations ranging from 1% to 2%.

For comparison, the identification was also performed by using the approach based on RMSE minimization. It is worth noting that the polytope algorithm requires an initial guess for the α, a, b parameters. In order to simulate uncertainty in this guess, the parameters were randomly initialized with uniform distribution over an interval of $\pm 50\%$ around the actual values. Compared to the proposed method, the optimization approach is more computationally intensive, owing to the need to simulate the fractional-order model in order to evaluate the cost function (i.e. the RMSE value) over successive iterations of the polytope algorithm. In order to investigate the trade-off between computational workload and accuracy of the parameter estimates, different upper bounds on the number of cost function evaluations (MaxFunEvals) were imposed in the polytope algorithm. The results are shown in Table 2 and Fig. 4. As expected, the identification outcome improves when the optimization approach is employed with larger number of cost function evaluations. However, the results are still worse than those obtained by the proposed method, which also benefits from a much smaller computational workload.

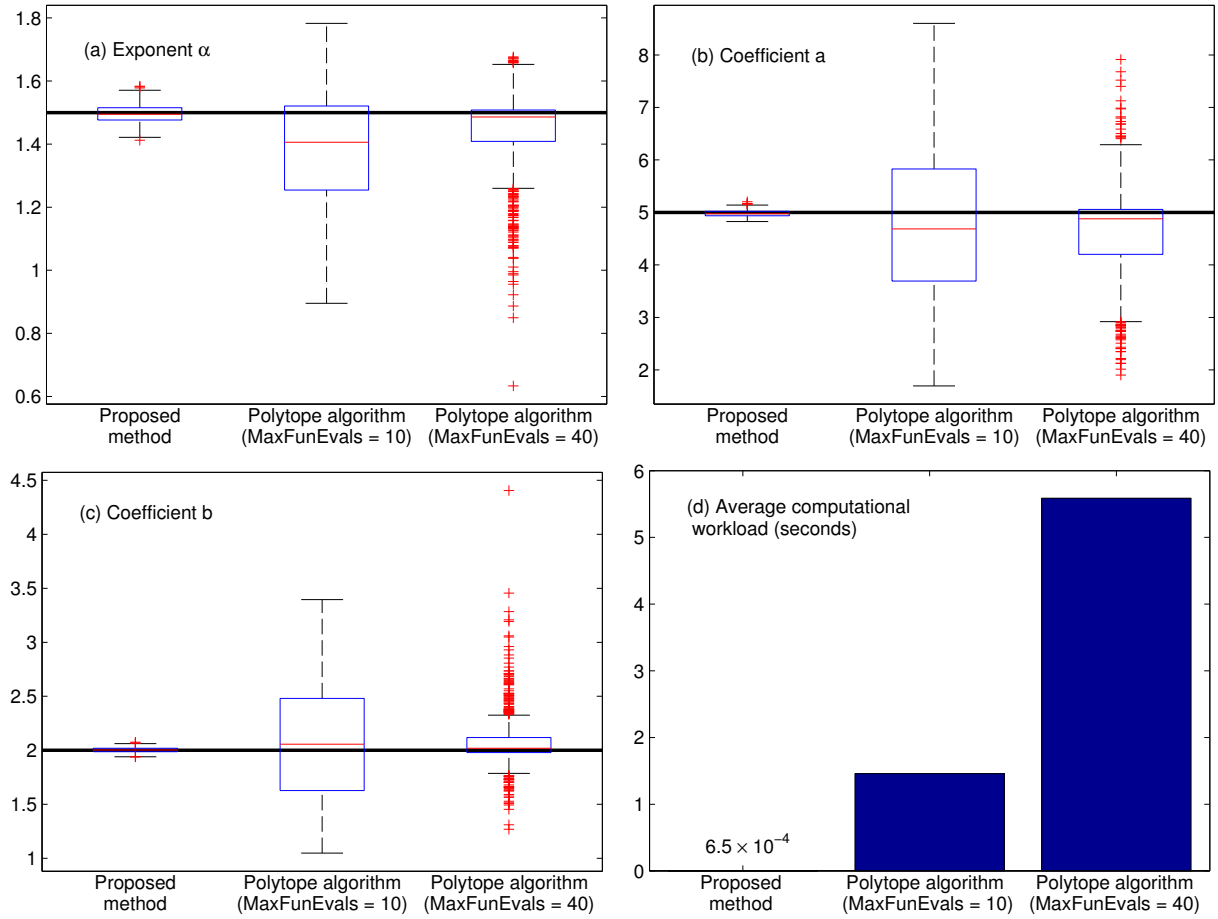

Figure 4: Example 1. Identification results obtained over 1000 realizations and average computational workload. The (a), (b), (c) boxplots present the median (central line), 25th and 75th percentiles (box edges), non-outlier extreme points (whiskers) and outliers (cross markers) of the data. The thick horizontal line indicates the actual parameter value.

5.2. Example 2

Consider a transfer function of the form (1) with $n = m = 1$, $b_0 = 2$, $b_1 = 3$, $a_1 = 5$, $\beta_1 = 0.5$ and $\alpha_1 = 1.5$. For brevity of notation, the fractional exponents β_1 and α_1 will be denoted simply by β and α, i.e.

$$G(s) = \frac{b_0 + b_1 s^{\beta}}{1 + a_1 s^{\alpha}} = \frac{2 + 3s^{0.5}}{1 + 5s^{1.5}} \tag{34}$$

The identification was carried out by using a pseudo-random binary signal $u(t)$, shown in Fig. 5a. As in the previous example, the output signal $y(t)$ was corrupted with additive Gaussian noise of zero mean and standard deviation of 0.1. The resulting signal is presented in Fig. 5b.

In this case, the calculation of $w(\infty)$ can be simplified, because the input signal has a piecewise constant profile of the form

$$u(t) = \begin{cases} u_0,\ 0 \le t < t_1 \\ u_j,\ t_j \le t < t_{j+1},\ j = 1, 2, \ldots, M-1 \\ u_M,\ t \ge t_M \end{cases} \tag{35}$$

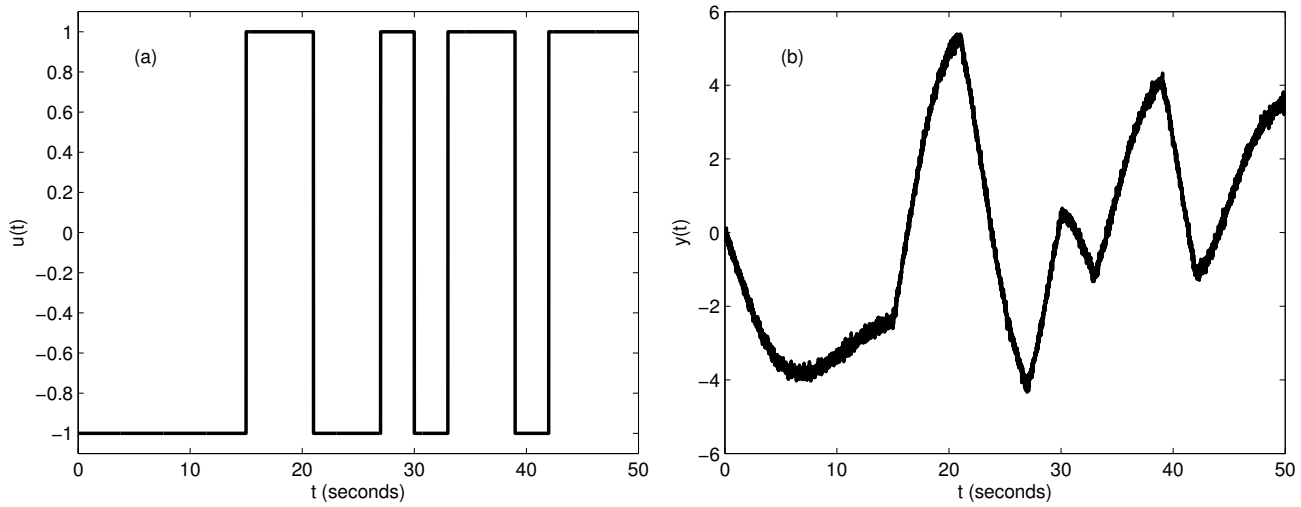

Figure 5: Example 2. (a) Input $u(t)$ and (b) output $y(t)$ signals employed in the identification.

where $t_j, j = 1, 2, \ldots M$, are the switching times and $u_j = (-1)^j, j = 0, 1, \ldots M$, are the input levels. In view of the block diagram in Fig. 1, it follows that

$$w(\infty) = \sigma \int_0^\infty u(\tau) e^{-\sigma\tau} d\tau = \sigma \left(u_0 \int_0^{t_1} e^{-\sigma\tau} d\tau + \sum_{j=1}^{M-1} u_j \int_{t_j}^{t_{j+1}} e^{-\sigma\tau} d\tau + u_M \int_{t_M}^\infty e^{-\sigma\tau} d\tau \right)$$

$$= u_0 \left(1 - e^{-\sigma t_1}\right) + \sum_{j=1}^{M-1} u_j \left(e^{-\sigma t_j} - e^{-\sigma t_{j+1}}\right) + u_M e^{-\sigma t_M} = u_0 + \sum_{j=1}^{M} (u_j - u_{j-1}) e^{-\sigma t_j} \tag{36}$$

Following the procedure proposed in Section 4, $q = 2(n + m + 1) = 6$ different values of σ were employed in the identification. In light of the rationale described in Example 1, the values $\sigma_1 = 2(\ln 100)/50 = 0.184$ and $\sigma_i = \sigma_1^{1/i}$, $i = 2, 3, \ldots, 6$ were adopted.

Fig. 6a presents a plot of the index E defined in (30) for a grid of α and β values ranging from 0.1 to 2.0 with 0.1 steps. A logarithmic scale for E is employed for better visualization. The grid search was restricted to β values smaller than α, in order to keep the transfer function $G(s)$ strictly proper. As can be seen in Fig. 6a, the index E is minimized for $\alpha = 1.5$ and $\beta = 0.5$, which correspond to the actual values of the fractional exponents in (34). For comparison, Fig. 6b presents the root-mean-square error (RMSE) between the noisy system output and the resulting model response for the tested α and β values. Again, the smallest RMSE was obtained for $\alpha = 1.5$ and $\beta = 0.5$. However, the evaluation of index E in the entire grid search procedure took approximately 0.25 second, whereas the RMSE evaluation took more than 30 seconds. In fact, the RMSE calculations require one simulation of the fractional-order model for each pair of α, β values in the search grid. In contrast, the evaluation of the index E defined in (30) is much simpler, as it only involves standard matrix operations. Such findings point to a major computational advantage of using index E in the search for the best fractional exponents, as compared to the use of RMSE adopted in [36].

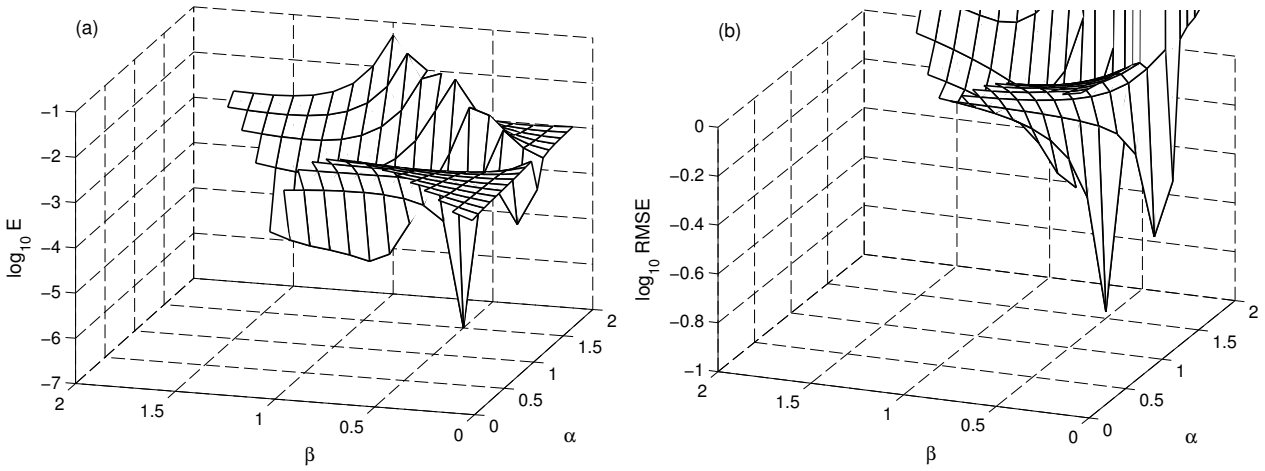

Figure 6: Example 2. (a) Index E employed in the choice of α and β. (b)Root-mean-square error (RMSE) between the model response and the noisy system output (vertical axis cropped for better visualization).

By using $\alpha = 1.5$ and $\beta = 0.5$, the identification resulted in the following transfer function:

$$G_{identified}(s) = \frac{2.0 + 2.9s^{0.5}}{1 + 4.9s^{1.5}} \tag{37}$$

which closely matches (31). As can be seen in Fig. 7, the response of the identified model is well inside the bounds of the noisy output signal. Indeed, as indicated by the minimum point in Fig. 6b, the root-mean-square error between these two signals is 10^{-1}, which corresponds to the standard deviation of the added noise.

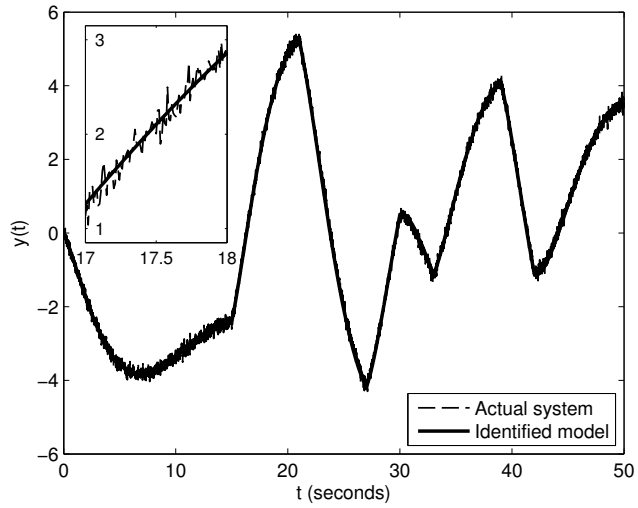

Figure 7: Example 2. Actual system response and output of the identified model. The inset is an enlarged view around $t = 17.5$ s.

Table 3: Example 2. Parameter estimates (average ± standard deviation over 1000 realizations) and computational workload. MaxFunEvals is the upper bound on the number of cost function evaluations in the polytope algorithm.

Parameter	Proposed method	Polytope algorithm		Actual value
		MaxFunEvals = 20	MaxFunEvals = 80	
α	1.51 ± 0.04	1.4 ± 0.2	1.5 ± 0.1	1.5
β	0.5 ± 0.1	0.5 ± 0.1	0.5 ± 0.2	0.5
a_1	4.9 ± 0.2	4.8 ± 1.1	4.8 ± 0.6	5
b_0	2.0 ± 0.4	2.1 ± 0.6	1.9 ± 0.5	2
b_1	3.0 ± 0.4	3.0 ± 0.9	2.8 ± 0.9	3
Average computational workload (seconds)	1.5	3.2	12.4	

As in the previous example, the reproducibility of the results was investigated by repeating the identification 1000 times, with different realizations of the measurement noise. In this investigation, a finer search grid was employed, with α and β values varying with 0.025 steps from 0.75 to 2.25 and 0.25 to 0.75, respectively, which correspond to intervals of $\pm 50\%$ around the actual exponent values. For comparison, the optimization approach was employed with random initialization of the α, β, a_1, b_0, b_1 parameters over an interval of $\pm 50\%$ around the actual values. The results are shown in Table 3 and Fig. 8 for two different upper bounds on the number of function evaluations (MaxFunEvals) in the polytope algorithm. As can be seen, even with MaxFunEvals = 80, the optimization approach is still outperformed by the proposed method regarding the average value and/or standard deviation of the parameter estimates.

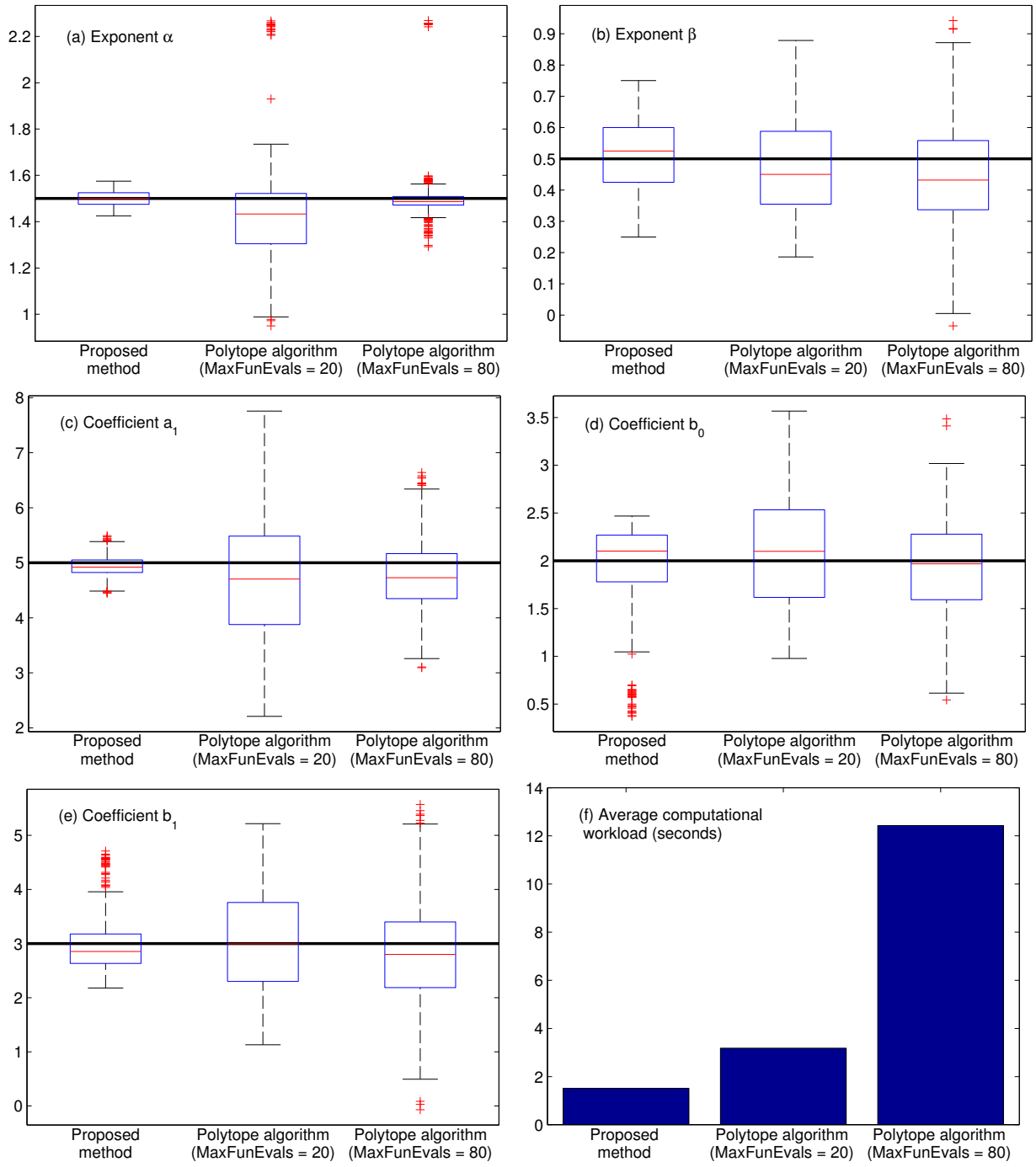

Figure 8: Example 2. Identification results obtained over 1000 realizations and average computational workload. The (a), (b), (c) boxplots present the median (central line), 25th and 75th percentiles (box edges), non-outlier extreme points (whiskers) and outliers (cross markers) of the data. The thick horizontal line indicates the actual parameter value.

6. Conclusion

This paper proposed a new identification method for fractional-order systems, which allows for the use of arbitrary input signals within an exponential modulation scheme. This contribution significantly extends the scope of application of a previous step-response formulation [36], which can actually be regarded as a simple particular case of the method proposed herein. For transfer functions of the form $G(s) = b/(1 + as^{\alpha})$, a newly derived formulation enabled the determination of the fractional exponent α and the coefficients a, b through the solution of a cubic equation. In the general case, a new evaluation index was proposed for the search of the best fractional exponents, as an alternative to the root-mean-square error (RMSE) between the model response and the system output [36]. The calculation of this new index does not require the simulation of the fractional order model, thus enabling a 100-fold reduction in computational workload (2.5×10^{-1} s as opposed to 3.0×10^{1} s) when compared to the RMSE evaluation. By means of simulation examples, the proposed method was shown to provide identification results in close agreement with the actual system parameters, even in the presence of measurement noise. In contrast, the results of an output-error optimization approach based on the polytope algorithm were generally less accurate, while at the same time required larger computational effort.

It is worth noting that the proposed method requires the system to be initially at rest. The handling of nonzero initial conditions is a relevant topic [40], which will be pursued in future studies. Future work could also be concerned with evaluation metrics other than the least-squares criterion employed in the present paper. Within this scope, using the absolute error may be a convenient choice in cases where the measurement noise has impulsive features [41]. Moreover, the extension to multiple input multiple output systems [42] and systems with time delay [43] should also be promising lines of investigation.

Acknowledgments

This work was supported by FAPESP (grants 2011/17610-0, 2011/13777-8) and CNPq (research fellowships 303393/2018-1, 309872/2018-9, 301227/2017-9). The authors are also grateful to Dr. Rubens J. M. Afonso (ITA) for granting access to the computational platform employed in this work.

References

[1] A. S. Elwakil, Fractional-order circuits and systems: an emerging interdisciplinary research area, IEEE Circuits and Systems Magazine 10 (4) (2010) 40–50.

[2] C. Ionescu, A. Lopes, D. Copot, J. A. T. Machado, J. H. T. Bates, The role of fractional calculus in modeling biological phenomena: A review, Communications in Nonlinear Science and Numerical Simulation 51 (2017) 141–159.

[3] C. Ionescu, J. F. Kelly, Fractional calculus for respiratory mechanics: Power law impedance, viscoelasticity, and tissue heterogeneity, Chaos Solitons & Fractals 102 (2017) 433–440.

[4] R. E. Gutiérrez-Carvajal, L. F. Melo, J. M. Rosário, J. A. T. Machado, Condition-based diagnosis of mechatronic systems using a fractional calculus approach, International Journal of Systems Science 47 (9) (2016) 2169 – 2177.

[5] R. S. Barbosa, J. A. T. Machado, I. S. Jesus, Effect of fractional orders in the velocity control of a servo system, Computers & Mathematics with Applications 59 (5) (2010) 1679–1686.

[6] C. Farges, L. Fadiga, J. Sabatier, Hinf analysis and control of commensurate fractional order systems, Mechatronics 23 (2013) 772–780.

[7] M. E. Fouda, A. S. Elwakil, A. G. Radwan, B. J. Maundy, Fractional-order two-port networks, Mathematical Problems in Engineering (2016) 5976301.

[8] I. S. Jesus, J. A. T. Machado, Development of fractional order capacitors based on electrolyte processes, Nonlinear Dynamics 56 (1-2) (2009) 45–55.

[9] M. S. Sarafraz, M. S. Tavazoei, Realizability of fractional-order impedances by passive electrical networks composed of a fractional capacitor and RLC components, IEEE Transactions on Circuits and Systems I: Regular Papers 62 (12) (2015) 2829 – 2835.

[10] A. G. Radwan, Resonance and quality factor of the $RL_\alpha C_\alpha$ fractional circuit, IEEE Journal on Emerging and Selected Topics in Circuits and Systems 3 (3) (2013) 377 – 385.

[11] B. Wang, Z. Liu, S. E. Li, S. J. Moura, H. Peng, State-of-charge estimation for lithium-ion batteries based on a nonlinear fractional model, IEEE Transactions on Control Systems Technology 25 (1) (2017) 3 – 11.

[12] C. Psychalinos, A. S. Elwakil, B. J. Maundy, A. Allagui, Analysis and realization of a switched fractional-order-capacitor integrator, International Journal of Circuit Theory and Applications 44 (11) (2016) 2035 – 2040.

[13] A. S. Elwakil, A. Allagui, T. J. Freeborn, B. J. Maundy, Further experimental evidence of the fractional-order energy equation in supercapacitors, AEU - International Journal of Electronics and Communications 78 (2017) 209–212.

[14] R. M. Hill, L. A. Dissado, R. R. Nigmatullin, Invariant behaviour classes for the response of simple fractal circuits, Journal of Physics: Condensed Matter 3 (48) (1991) 9773–9790.

[15] R. R. Nigmatullin, Theory of dielectric relaxation in noncrystalline solids: from a set of micromotions to the averaged collective motion in the mesoscale region, Physica B: Condensed Matter 358 (1-4) (2005) 201–215.

[16] J. A. T. Machado, I. S. Jesus, A. Galhano, J. B. Cunha, Fractional order electromagnetics, Signal Processing 86 (10) (2006) 2637–2644.

[17] R. Garrappa, Grunwald-Letnikov operators for fractional relaxation in Havriliak-Negami models, Communications in Nonlinear Science and Numerical Simulation 38 (2006) 178–191.

[18] F. Mainardi, R. Garrappa, On complete monotonicity of the Prabhakar function and non-Debye relaxation in dielectrics, Journal of Computational Physics 293 (2015) 70–80.

[19] F. Mainardi, Fractional calculus and waves in linear viscoelasticity, Imperial College Press, London, 2010.

[20] A. Giusti, On infinite order differential operators in fractional viscoelasticity, Fractional Calculus and Applied Analysis 20 (4) (2017) 854–867.

[21] A. Giusti, I. Colombaro, Prabhakar-like fractional viscoelasticity, Communications in Nonlinear Science and Numerical Simulation 56 (2018) 138–143.

[22] D. Sierociuk, A. Dzielinski, G. Sarwas, I. Petras, I. Podlubny, T. Skovranek, Modelling heat transfer in heterogeneous media using fractional calculus, Philosophical Transactions of the Royal Society A 371 (2013) 20120146.

[23] I. S. Jesus, J. A. T. Machado, Fractional control of heat diffusion systems, Nonlinear Dynamics 54 (3) (2008) 263–282.

[24] I. S. Jesus, J. A. T. Machado, R. S. Barbosa, Control of a heat diffusion system through a fractional order nonlinear algorithm, Computers & Mathematics with Applications 59 (5) (2010) 1687–1694.

[25] N. Aguila-Camacho, M. A. Duarte-Mermoud, J. A. Gallegos, Lyapunov functions for fractional order systems, Communications in Nonlinear Science and Numerical Simulation 19 (2014) 2951–2957.

[26] Z. Gao, Robust stability criterion for fractional-order systems with interval uncertain coefficients and a time-delay, ISA Transactions 58 (2015) 76–84.

[27] B. B. Alagoz, Hurwitz stability analysis of fractional order LTI systems according to principal characteristic equations, ISA Transactions 70 (2017) 7–15.

[28] B. Wang, J. Xue, F. Wu, D. Zhu, Robust Takagi-Sugeno fuzzy control for fractional order hydro-turbine governing system, ISA Transactions 65 (2016) 72–80.

[29] E. Keshavarz, Y. Ordokhani, M. Razzaghi, A numerical solution for fractional optimal control problems via Bernoulli polynomials, Journal of Vibration and Control 22 (2016) 3889–3903.

[30] L. V. Hien, C. T. Kinh, Decentralised stabilisation of positive fractional-order interconnected systems, IET Control Theory and Applications 11 (2017) 2391–2395.

[31] R. Malti, M. Aoun, J. Sabatier, A. Oustaloup, Tutorial on system identification using fractional differentiation models, in: Proc. 14th IFAC Symposium on System Identification, Newcastle, Australia, 2006, pp. 606–611.

[32] Y. Q. Chen, I. Petras, D. Xue, Fractional order control - A tutorial, in: Proc. American Control Conference, St. Louis, USA, 2009, pp. 1397–1411.

[33] D. Idiou, A. Charef, A. Djouambi, Linear fractional order system identification using adjustable fractional order differentiator, IET Signal Processing 8 (2014) 398–409.

[34] Y. Li, X. Meng, B. Zheng, Y. Ding, Parameter identification of fractional order linear system based on Haar wavelet operational matrix, ISA Transactions 59 (2015) 79–84.

[35] M. Tavakoli-Kakhki, M. S. Tavazoei, Estimation of the order and parameters of a fractional order model from a noisy step response data, Journal of Dynamic Systems, Measurement, and Control 136 (3) (2014) 031020.

[36] L. A. Jacyntho, M. C. M. Teixeira, E. Assunção, R. Cardim, R. K. H. Galvão, S. Hadjiloucas, Identification of fractional-order transfer functions using a step excitation, IEEE Transactions on Circuits and Systems II: Express Briefs 62 (9) (2015) 896–900.

[37] G. F. Franklin, J. D. Powell, A. Emami-Naeini, Feedback Control of Dynamic Systems, 5th Edition, Prentice-Hall, Upper Saddle River, 2006.

[38] C. P. Li, W. H. Deng, D. Xu, Chaos synchronization of the Chua system with a fractional order, Physica A 360 (2006) 171–185.

[39] P. E. Gill, W. Murray, M. H. Wright, Practical Optimization, Academic Press, New York, 1981.

[40] Y. Lu, Y. Tang, X. Zhang, S. Wang, Parameter identification of fractional order systems with nonzero initial conditions based on block pulse functions, Measurement (In Press).

[41] R. Cui, Y. Wei, S. Cheng, Y. Wang, An innovative parameter estimation for fractional order systems with impulse noise, ISA Transactions 82 (2018) 120–129.

[42] D. Xue, T. Li, An approach to design controllers for MIMO fractional-order plants based on parameter optimization algorithm, ISA Transactions 82 (2018) 145–152.

[43] Y. Tang, N. Li, M. Liu, Y. Lu, W. Wang, Identification of fractional-order systems with time delays using block pulse functions, Mechanical Systems and Signal Processing 91 (2017) 382–394.